Applied Catalysis B: Environmental 127 (2012) 11–17

Contents lists available at SciVerse ScienceDirect

Applied Catalysis B: Environmental

journal homepage: www.elsevier.com/locate/apcatb

Adjustable kinetics in heterogeneous photocatalysis demonstrating the relevance of electrostatic interactions

Jan Ungelenk, Claus Feldmann*

Karlsruhe Institute of Technology (KIT), Institut für Anorganische Chemie, Engesserstraße 15, D-76131 Karlsruhe, Germany

ARTICLE INFO

Article history:
Received 11 April 2012
Received in revised form 24 July 2012
Accepted 31 July 2012
Available online 10 August 2012

Keywords:
Photocatalysis
Kinetics
Electrostatic interaction
In situ measurement
Tin tungstate

ABSTRACT

The performance of a photocatalyst depends on a complicated correlation of a multitude of parameters including extrinsic ones. Among, the pH value is probably the most important parameter. Gaining a detailed knowledge of the underlying processes still represents a major challenge but is required to optimize known or to develop efficient novel photocatalysts. Here, we present a favorable model system comprising nano-β-$SnWO_4$ as the photocatalyst and azo-dyes in different charge states. Disentangling parameters, we demonstrate that the reaction order of our exemplary photocatalytic degradation reaction can be fully tuned from first over zero- to mixed-order by simply adjusting the pH. Thereby we elucidate the importance of electrostatic interactions which are of significance to various aspects including: the decomposition of non-charged persistent pollutants, the inactivation of bacteria as well as the influence of electrolyte containing media, the polarity of the solvent or of specific crystal facets. Based on our results, we suggest taking the electric double layer on the photocatalyst into account. This multi-component view reconciles reported contradictions and allows interpreting results that have been intriguing or misunderstood so far.

1. Introduction

Photocatalysis has become a most significant research field owing to its enormous potential on the one hand, and to the pressing global environmental problems on the other hand. Many publications are focused on maximizing the activity of a certain photocatalyst by, for instance, extending its absorption range [1], enhancing its crystallinity [2,3], enlarging its specific surface [4] or optimizing its shape [3,5].

A high photocatalytic activity is, however, not a single material property but depends on a multitude of parameters, including extrinsic ones, which are governed by the environment and the given conditions. Thus, a photocatalyst may exhibit a high activity for a certain reaction, but it may be almost inactive for another reaction or for the same reaction, if conducted under slightly different conditions. Moreover, the most relevant parameters are strongly coupled with each other. Therefore, it is a major challenge to interpret or – even better – to predict the kinetics of heterogeneous photocatalytic reactions. In sum, a detailed knowledge of all influencing parameters is required for further optimization of known or development of novel photocatalysts. Such knowledge is even more important when optimizing a photocatalyst for a special purpose like photodisinfection, water detoxification or driving a specific reaction of a selected reactant from a mixture of reactants. Therefore, a method to disentangle the plurality of variables and to get a better understanding of their essential influence is still urgently sought-after [6].

So far, detailed knowledge is lacking, since: (1) the established model-reactions do not simulate realistic scenarios; (2) there is no robust model-reaction system available, which tolerates major changes in the chemical surrounding; (3) the prevailing mechanistic description is insufficient.

The most *common testing method* – the decomposition of a highly diluted cationic or anionic dye – is not representative for non-charged reactants and/or degradation reactions in media containing electrolytes or a mixture of various reactants. Note, that non-charged reactants represent a most significant group, comprising many commodities and persistent pollutants (*e.g.*, dioxins, polycyclic aromatic hydrocarbons, nitrosamines).

Most *photocatalysts* change significantly upon changing conditions impeding clear-cut kinetic studies. TiO_2, as the most studied photocatalyst, for instance changes its surface charge from positive to negative when going from acidic to basic milieu. Thus, its zeta-potential exhibits a strong gradient, and TiO_2 is non-charged to weakly charged and unstable against agglomeration and sedimentation in the neutral region [7].

In the *prevailing mechanistic description* – *viz.* a monomolecular Langmuir–Hinshelwood (L–H) mechanism – the activity of a photocatalyst is assumed to be only dependent of the surface coverage

* Corresponding author. Tel.: +49 721 608 42855.
E-mail address: claus.feldmann@kit.edu (C. Feldmann).

0926-3373/$ – see front matter © 2012 Elsevier B.V. All rights reserved.
http://dx.doi.org/10.1016/j.apcatb.2012.07.037

of the regarded reactant. This view is limited to first- (incomplete coverage) or zero-order (full coverage) kinetics [8]. No other than exponential or linear decays, or mixtures of them, can be explained. But even in these simple cases, the simplified L–H model frequently fails to explain experimental data or leads to paradoxical conclusions [9].

In this publication, we present a favorable model-reaction system comprising nano-β-$SnWO_4$ as the photocatalyst as well as differently charged azo-dyes as model-compounds. This reaction system allows for collecting a multitude of data points *via in situ* measurement and disentangling of parameters. We demonstrate that the kinetics of these exemplary degradation reactions is pH dependent and thus adjustable. Thereby, we elucidate the influence of electrostatic interactions of degradation reactions in heterogeneous photocatalysis, which are of significant importance for various aspects. This includes: the decomposition of non-charged persistent pollutants, the elimination of bacteria as well as the use of electrolyte-containing water as reaction medium. Based on our results, we suggest taking the electric double layer on the photocatalyst into account. This multi-component view reconciles reported contradictions and allows interpreting results that have been intriguing so far. Moreover, influences of the polarity of specific crystal facets of the photocatalyst or the polarity of the solvent can now be understood.

2. Experimental

2.1. Challenges of experimental methods

The most common way of monitoring a degradation reaction is to suspend the photocatalyst in a solution of an organic dye – the model compound – in pure water, to stir this mixture in the dark until an adsorption–desorption equilibrium is established, to illuminate this batch and to take samples after certain time intervals. From these samples the photocatalyst is removed by centrifugation or filtration, and the remaining concentration of the dye is analyzed with a spectrophotometer.

However, doing so is a non-automated, *ex situ* approach, which generates only limited data points, thus the validity of a corresponding kinetic analysis is rather poor. The actual measurement might be distorted by interfering processes, including non-photocatalytic side reactions (*e.g.*, photolysis of the dye or bleaching owing to leuco-forms), adsorption (*e.g.* to filters), agglomeration and sedimentation of the photocatalyst or scattering at residual photocatalyst particles. Moreover, all these processes are influenced by a complex interplay of parameters, with the pH being the most important one [6,10]. The pH-value governs the charge of the reactant as well as the surface charge of the photocatalyst and thereby influences the electrostatic interaction between photocatalyst and the reactant (*i.e.* adsorption) as well as between the particles of the photocatalyst (*i.e.* agglomeration and thereby available surface, sedimentation, scattering). Furthermore, chemical reactions may be influenced by the pH as well: at basic conditions the photo-generation of hydroxyl radicals is facilitated [10], whereas at acidic conditions the redox activity of the dyes is affected [11], *e.g.*, due to protonated carbonyl- or azo-groups. All these aspects impede clear-cut kinetic studies, so far, especially kinetic studies in dependence of the pH-value.

2.2. A favorable model-system and experimental set-up

Here, we address these challenges (*cf.* Section 2.1) in developing a versatile model-reaction system, comprising several differently charged azo-dyes as *model compounds* and nano-β-$SnWO_4$ as the *photocatalyst.*

Model compounds: We have chosen the azo-dyes methyl orange and disperse black 3 as suitable model compounds. Both dyes are very resistant to light and cannot be transformed to leuco-forms, excluding photolysis or reductive bleaching (*cf.* Supporting information). Moreover, these dyes have the same parental structure but can adopt three different charge states all within the acidic and therefore the same pH-milieu: cationic, zwitterionic and anionic (Fig. 1B). In the following the dyes are denoted as cationic, zwitterionic and anionic dye.

Photocatalyst: High-quality nanoparticles of β-$SnWO_4$ are attractive for kinetic studies due to their properties, which we reported earlier [3,12]: a high daylight-activity, a small mean diameter ($d \leq 20$ nm) and an almost constant negative surface-charge ($\zeta \leq -40$ mV) over a wide pH-range. For further details regarding nano-β-$SnWO_4$ see [3,12] as well as Supporting information.

Note the following resulting advantages:

(1) According to the flat gradient of its zeta-potential, the pH value of the suspension can be varied over a wide range, adjusting the charge of a reactant, without changing the surface-charge of the β-$SnWO_4$ nanoparticles, which allows studying different electrostatic interactions.
(2) Due to the small diameter and the stability of the β-$SnWO_4$ nanoparticles, scattering effects are minimized and do not vary over time. Nanoparticles with these properties are denoted as transparent nanoparticles [6], and allow *in situ*-measurements of degradation reactions, without removing the photocatalyst. Thus, the whole suspension is continuously pumped through a spectrometer (Varian Cary 100) by a peristaltic pump and returns in the illuminated beaker (Fig. 1A). By doing so, every second a data point can be collected instead of only collecting few data points per hour.
(3) Real environments usually contain electrolytes, which are detrimental for colloidal stability. Owing to its efficient electrostatic stabilization, β-$SnWO_4$ nanoparticles, however, are remarkably stable against agglomeration and sedimentation, allowing for studies in electrolyte-containing media. Even when suspended in phosphate-buffered saline, simulating biological environments, nanoparticles of β-$SnWO_4$ are stable against centrifugation up to 20,000 rpm for 20 min.

2.3. Photocatalytic characterization

We studied the photocatalytic degradation over nano-β-$SnWO_4$ (Fig. 2A) as well as the adsorption on nano-β-$SnWO_4$ (Fig. 2B) for each dye, by recording the absorption at their particular absorption-band maxima (cationic λ_{max} = 470 nm, zwitterionic λ_{max} = 508 nm, anionic λ_{max} = 466 nm), under equal conditions, but varying the pH to adjust the charge state (293 K, 25 mL suspension, c (nano-β-$SnWO_4$) = 1.25×10^{-3} M, c (dye) = 2×10^{-5} M, lamp: Osram Xenophot HLX 64634 (3300 K) halogen bulb). Adsorption and degradation experiments were conducted in 1:10 diluted phosphate-buffered saline to simulate surface water.

2.4. Synthesis

Nano-β-$SnWO_4$ was synthesized by a route slightly modified from our previous synthesis [3,12]. In a typical recipe, $SnCl_2$ (417.1 mg, 2.2 mmol) was dissolved in 2.5 mL of deionized water. Under vigorous magnetic stirring, this solution was added to 2.5 mL of an equimolar aqueous solution of $Na_2WO_4 \cdot 2H_2O$ (725.7 mg) at ambient temperature. A bright yellow nanomaterial was generated and the resulting suspension was directly diluted with 20 mL of freshly prepared phosphate-buffered saline (8.0 g L^{-1} NaCl, 0.2 g L^{-1} KCl, 1.44 g L^{-1} Na_2HPO_4, 0.24 g L^{-1} NaH_2PO_4 in distilled water). The obtained suspensions were destabilized with

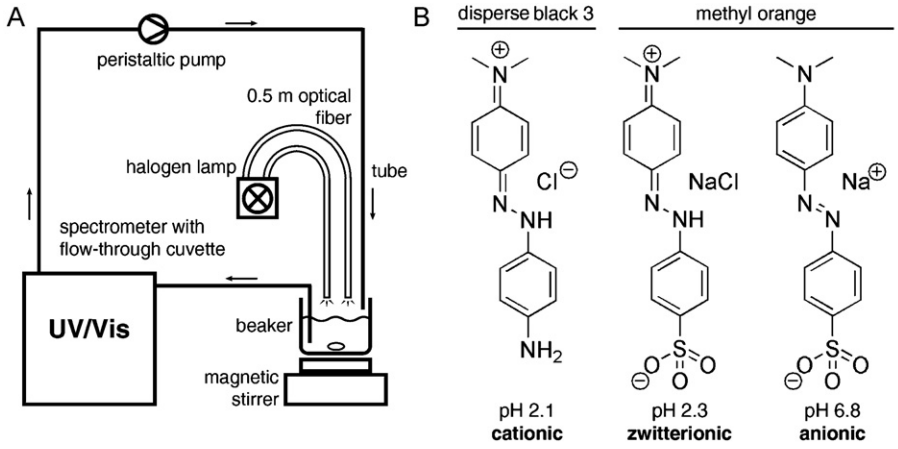

Fig. 1. (A) Experimental set-up for continuous *in situ* photocatalytic activity tests; (B) structural formula and charge state of the used dyes.

ethanol, centrifuged (15 min, 25,000 rpm) and redispersed two times for washing. Finally, the β-$SnWO_4$ nanoparticles were redispersed in phosphate-buffered saline and centrifuged for 2 min at 10,000 rpm to remove agglomerates. The resulting supernatants were stable suspensions of nano-β-$SnWO_4$ having a concentration of 4 g L^{-1} (*cf.* [3,12] and Supporting information for detailed characterization).

3. Results and discussion

In the following, the three dyes (*i.e.*, cationic disperse black 3, zwitterionic methyl orange, anionic methyl orange) were studied in view of their photodegradation under similar experimental conditions with nano-β-$SnWO_4$ as the applied photocatalyst. Despite their common parental structure, completely different degradation curves (Fig. 2A) and adsorption isotherms (Fig. 2B, *cf.* Supporting information) were observed for each dye, which are discussed in the following in the order cationic, zwitterionic and anionic dye.

3.1. Cationic dye

The cationic dye showed an exponential decay for the degradation curve (Fig. 2A) and its adsorption isotherm was of Henry-type, *i.e.* no saturation is observed (Fig. 2B). The linear relation of the Henry-isotherm indicates further that the amount of adsorbed dye is directly proportional to the concentration of the dye in feed, thus the monomolecular L–H-mechanism may be applied here [8]. In accordance with monomolecular L–H-kinetics, a high but incomplete adsorption leads to a reaction of first-order, and thus to an exponential decaying degradation curve. Despite a strong attractive electrostatic interaction between the negatively charged photocatalyst and the cationic dye, no saturation can be observed even at high dye concentrations. These results confirm the high photocatalytic activity of nano-β-$SnWO_4$ under simulated daylight as well as its high specific surface [3,12].

3.2. Zwitterionic dye

In contrast to the cationic dye, the adsorption isotherm of the zwitterionic dye showed a saturation plateau (Fig. 2B), and the degradation curve was linear over a wide range (Fig. 2A). If we had not conducted further experiments, these results would appear to be consistent with the monomolecular L–H-mechanism, assuming full coverage of the dye as demonstrated by its adsorption isotherm resulting in zero-order degradation independent of the reactant's concentration. This apparent clearness might be a reason that a monomolecular L–H-mechanism is presumed in many publications without experimental evidence [8]. It is however counterintuitive that the zwitterionic dye should be fully adsorbed, although no strong attractive electrostatic interaction is to be expected owing to the formally neutral charge state of the dye. Indeed, comparison of the adsorption isotherms shows explicitly that much less

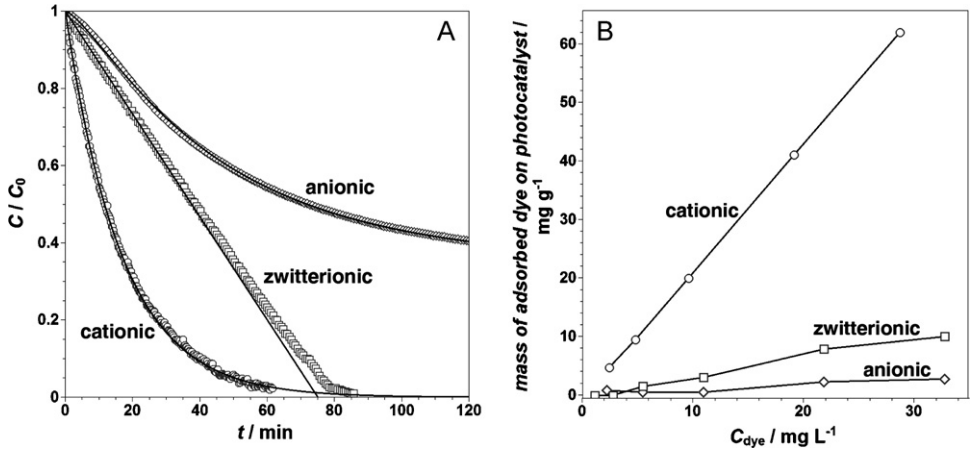

Fig. 2. (A) Photocatalytic degradation curves of cationic, zwitterionic and anionic dye over β-$SnWO_4$ and best fits (for the first 20 min in case of the zwitterionic dye, *cf.* Supplementary data) of that curves; (B) adsorption isotherms of cationic, zwitterionic and anionic dye of the same parental structure over the same photocatalyst (β-$SnWO_4$) under equal conditions (only pH and anchor groups are changed, *cf.* Fig. 1B).

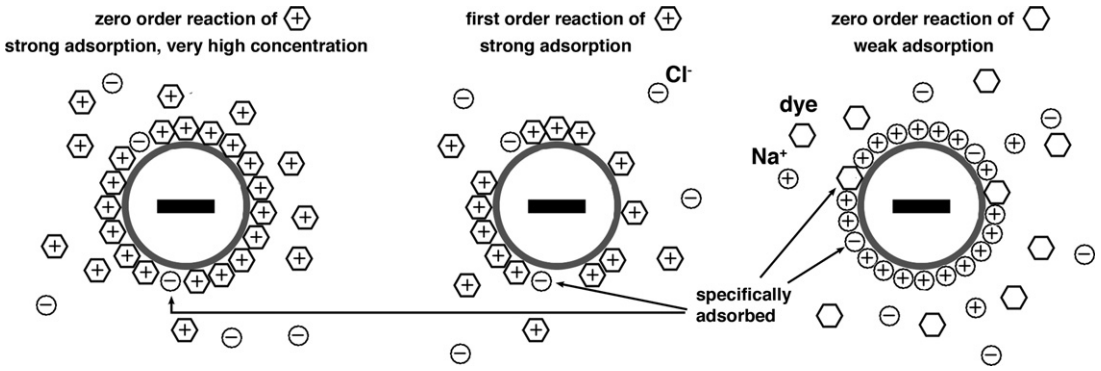

Fig. 3. The electric double layer on a negatively charged photocatalyst-particle depending on the concentration and the charge state of the dye. The first scheme refers to full coverage and resulting zero-order reaction according to the simplified L–H-mechanism. The last scheme shows, however, that also weak adsorption might result in zero-order reaction.

zwitterionic dye was adsorbed on the negatively charged photocatalyst than of the cationic dye. The cationic dye, however, did not completely cover the photocatalyst's surface as discussed above.

This finding is analogous to the *kinetic-order paradox* which has been encountered by Aramendía et al. [9], while they were studying the photocatalytic degradation of chlorinated pyridines over TiO_2. The authors found *ortho*-chloropyridine to obey first-order and *meta*-chloropyridine to obey zero-order kinetics, respectively. According to the L–H-mechanism, these findings indicate incomplete (*o*-chloropyridine) and full (*m*-chloropyridine) coverage of TiO_2. In contrast to this expectation, adsorption experiments clearly demonstrated that the adsorption of *o*-chloropyridine to TiO_2 is much stronger than the adsorption of *m*-chloropyridine [9].

In our opinion, the failure of the simplified, monomolecular L–H-mechanism, which is commonly used in photocatalysis, lies in its oversimplification: it takes only the reactant into account. There is only one scenario, however, where this situation applies: if the reactant is identical with the solvent like, for instance, when photocatalytically degrading pure isopropanol [13]. But even in such a case there are actually several species when also considering degradation products. As a matter of fact, there have been attempts to expand the monomolecular L–H-mechanism by adding a term for the solvent [14], but this approach is of limited feasibility: Think of a solution containing i species (*e.g.*, solvent, reactant, co- and counter-ions, degradation products or competing reactants). For each species a term would have to be added, ending up with an equation of $2i$ parameters (*i.e.*, an adsorption term and the concentration for each species) that have to be known or determined.

From our point of view, a much better approach is therefore to describe the adsorption behavior of several species based on statistics rather than discretely. Fortunately, such a statistic description is already available with the concept of the electric double layer [15]: According to these concepts, a cationic dye, as discussed in the section above, will strongly adsorb on negatively charged nanoparticles (*i.e.* the photocatalyst) forming the so called Stern layer. Thus, the monomolecular L–H-mechanism will be applicable in such cases (Fig. 3). In contrast, a zwitterionic dye, as discussed in this section, will not form a Stern layer on a negatively charged photocatalyst but its counterions do, *i.e.* Na^+ in the case of methyl orange (Fig. 3). Nevertheless, the actual dye, *i.e.* the zwitterionic organic moiety, adsorbs – to a certain extent – specifically due to van der Waals forces [15]. Taking this concept figuratively, not the whole surface is available for the zwitterionic dye but only distinct "pockets" within the Stern layer, which is built up of the Na^+ counterions of the zwitterionic dye (and of further suitable species, if available) with the total number of these "pockets" being governed by statistics.

This view reconciles the apparent contradiction that saturation can be observed while the overall adsorption is low, since only the available "pockets" have to be completely saturated rather than the whole specific surface of the photocatalyst. Thus, in contrast to prevailing expectations, *weak* rather than *strong* adsorption may lead to zero-order kinetics. Taking this picture for granted, the kinetics of the zwitterionic dye regarded here (and of non-charged reactants in general) should be describable analogous to enzyme-kinetics (*cf.* Supporting information), where – according to Michealis and Menten (Eq. (1)) – a substrate (*here*: the dye) binds to a specific pocket of an enzyme (*here*: statistically given amount of binding sites in the Stern layer). This approach is mathematically consistent with classical L–H-kinetics and must give a linear correlation in a C_0/v_0 *versus* C_0 plot (*cf.* Supporting information), which is a linearized form of the Michealis–Menten kinetics (Hanes–Woolf plot) [16], where C_0 are chosen different initial concentrations of the reactant and v_0 is the corresponding initial reaction velocity. Moreover, the reaction order must change from zero to one at low concentrations, *i.e.* the linear correlation of the C_0/v_0 *versus* C_0 plot must exhibit a non-zero intercept (*cf.* Supporting information).

Fig. 4A shows degradation curves of the zwitterionic dye for different initial concentrations. At the first glance, the widely linear curves are parallel, indicating that the reaction rate is independent of the initial concentration C_0, as typical for a zero-order reaction. To determine the corresponding initial reaction velocities v_0, which are not influenced by degradation products, a linear fit was applied to the first 60 s of each degradation curve (*cf.* inset in Fig. 4A). Fig. 4B shows a C_0/v_0 *versus* C_0 plot: Indeed, the obtained data are in very good agreement to a linear relation with a non-zero intercept (inset Fig. 4B), pointing to a change of the reactant order from zero to one. Note that the degradation curve shown in Fig. 2A has been fitted with a linear function from 0 to 20 min with very good agreement, too. Nonetheless the whole degradation curve resembles rather a curve resulting from the addition of this linear fit and of the exponential fit performed on the degradation curve of the cationic dye, which also demonstrates the change of the reaction order from zero to one at low concentrations.

The concept of treating the kinetics of the zwitterionic dye mathematically analogous to enzyme kinetics can be further verified by directly plotting v_0 (obtained *via* linear regression as shown in Fig. 4) *versus* C_0, the chosen initial dye concentration, which must lead to a hyperbolic saturation curve, described by Eq. (1). Herein, k represents the maximal reaction rate at full saturation. K is equal to the concentration of reactant at 50% saturation of statistical available binding sites (*cf.* Supporting information):

$$v_0 = \frac{k \cdot C_0}{K + C_0} \quad (1)$$

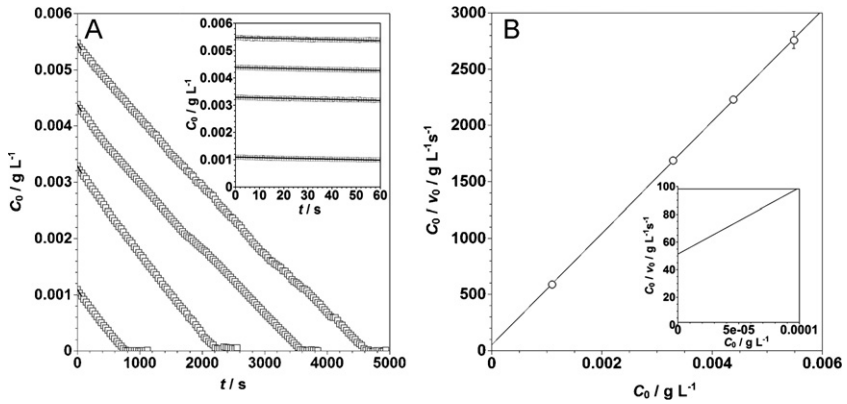

Fig. 4. (A) Degradation curves of the zwitterionic dye with different initial concentrations C_0 and linear fits of the first 60 s of each degradation curve (inset A, *cf.* supplementary data) to gain the initial reaction velocities v_0, and (B) C_0/v_0 *versus* C_0 Hanes–Woolf-plot with a linear fit showing a non-zero-intercept (inset B, *cf.* Supplementary data).

As shown in Fig. 5, non-linear regression analysis indeed gives a result within the limits of the errors which are given from the linear fits that are shown in Fig. 4A.

Altogether, all data and its analysis (Figs. 4 and 5, *cf.* Supporting information) support the suggested view. Zero-order kinetics has already been found for a multitude of non-charged reactants, including (halogenated) pyridines [17], phenols [18] and benzenes [19], as well as nitrosamines [20]. Note that these compounds represent commodities and can serve as model compounds for persistent pollutants (*e.g.*, dioxins, polycyclic aromatic hydrocarbons or nitrosamines), thus non-ionic reactants are of major importance. Still, an explanation for their zero-order kinetics has been missing so far.

3.3. Anionic dye

The anionic dye exhibited a sigmoidal degradation curve (Fig. 2A) and an adsorption isotherm similar to the adsorption isotherm of the zwitterionic dye (Fig. 2B). Although, saturation is reached again, less anionic dye is adsorbed than in its zwitterionic form as indicated by the lower saturation plateau (Fig. 2B). This finding is contradictive with respect to the simplified, monomolecular L–H-model, but in accordance with the concept suggested here: just similar to its zwitterionic form the negatively charged dye adsorbs to the negatively charged photocatalyst particles only due to van der Waals forces, but to a lesser extent than the zwitterionic form owing to the repulsive electrostatic interaction.

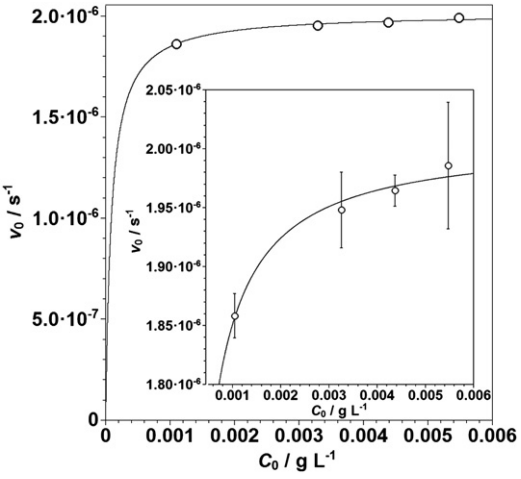

Fig. 5. Plot of initial reaction velocities v_0 *versus* the initial reactant concentration C_0 and fit (*cf.* Supplementary data) obtained from non-linear regression analysis according to Eq. (1).

Although sigmoidal degradation curves are common for many processes, they are surprisingly rarely identified in dye-degradation reactions over heterogeneous photocatalysts (which might in some cases be owing to a lack of sufficient data points) or – if noticed – not commented on [21], including our own earlier publication [12]. This deficit of awareness might be due to the fact, that sigmoidal curves cannot be explained by the prevailing monomolecular L–H-mechanism.

Remarkably, sigmoidal degradation curves are, nonetheless, absolutely common in the kinetics of photo-disinfection [22], *i.e.* the photocatalytic degradation of bacteria, described by empirical equations, with the Hom model being the most common one [23]:

$$C = \frac{C_0}{e^{k_1}(1 - e^{-k_2 t})^{k_3}} \quad (2)$$

From the chemical point of view, however, there is no difference whether the reactant is a single molecule or a molecule located at a bacterium. Indeed, a non-linear fit using the Hom equation (Eq. (2)) is in very good agreement with the observed data for the degradation curve of the anionic dye (Fig. 2A).

Sigmoidal decays are common for complex reactions, multiple interfering reactions and/or reactions showing a positive feedback like autocatalytic reactions. Such a positive feedback is given in photodisinfection, too. The most relevant bacteria exhibit a negatively charged cell membrane since negatively charged groups predominate on it, including, carboxylates, polysaccharides and phosphonates. For that reason, a photocatalyst is the more suitable for photodisinfection the higher its isoelectric point (*iep*) is [24]. By far the most photocatalysts, however, show an *iep* in the neutral or acidic region. Thus, for electrostatic reasons as discussed above, many photocatalysts show low adsorption on bacteria. During the photocatalytic reaction, however, the negatively charged cell membrane is attacked by photogenerated radicals, *i.e.* reactive oxygen species (ROS), and finally degraded [23,25]. The removal of the cell membrane leads to an acceleration of the photodisinfection reaction for two reasons: (1) the electrostatic repulsion is ceased, and (2) without their protective membrane the bacteria are less resistant to reactive oxygen species [25].

Interestingly there is an analogous situation for the anionic dye used in this study. In the first stage, the degradation reaction proceeds very slowly for similar electrostatic reasons. During the reaction, however, the pH value declines as shown in Fig. 6. Supposing its complete decomposition, each molecule of methyl orange (MO) generates up to 4 protons (*Eq. 3*):

$$(\mathrm{MO}) + 21.5\mathrm{O_2} \rightarrow 14\mathrm{CO_2} + 3[\mathrm{NO_3}]^- + [\mathrm{SO_4}]^{2-} + 5\mathrm{H_2O} + 4\mathrm{H^+} \quad (3)$$

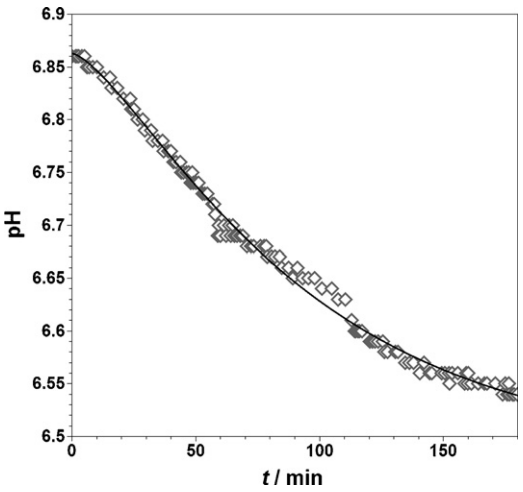

Fig. 6. Plot of pH *versus* time during the degradation reactions of the anionic dye and fit (*cf.* Supplementary data) obtained from non-linear regression analysis using the Hom-equation (2).

These protons may protonate the azo-group of methyl orange yielding its zwitterionic form (*cf.* Fig. 1B). Hence there are similar reasons for an acceleration of the degradation reaction as compared to bacteria: (1) electrostatic repulsion is ceased, and (2) the concentration of protonated dye at the photocatalyst's surface and within the diffusion length of reactive oxygen species is increased (*cf.* Fig. 2B). At the end, the attack of radicals is getting more effective again. Altogether, sigmoidal curves can also be understood with our model of taking the electric double layer on the surface of photocatalysts into account.

3.4. Significance of the results to various aspects

The concept suggested here of taking the electric double layer into account is of significance for every reaction where electrostatics can be influenced or does matter:

First of all, adjusting a suitable charge is clearly a means to optimize a photocatalytic reaction, as has been shown in this publication for the model compound methyl orange: the efficiency of its degradation was significantly enhanced by varying the pH, *i.e. by* changing the reaction order. Varying the pH, might also be used to achieve a preferential photocatalytic reaction of a specific isomer, if the acidities of the isomers differ. To this concern, *ortho*-(pKa_1 0.72) and *meta*-chloropyridine (pKa_1 2.72) [26] as well as *ortho*- (pKa_1 8.48) and *meta*-chlorophenol (pKa_1 9.08) [27] may represent relevant examples of constitutional isomers. In addition, fumaric (pKa_1 3.0) and maleic acid (pKa_1 1.9) may serve as examples representing *cis–trans* isomerism [28].

Recently great attention has been paid to faceted microcrystals of photocatalytic materials that are fully enclosed by highly reactive facets and exhibit a significantly enhanced activity [5]. Studying the photocatalytic activity of faceted ZnO microcrystals, Kislov et al. encountered that methyl orange, as a model compound, followed first-order reactions over the polar faces (ZnO(0 0 0 1)-Zn and ZnO(0 0 0 −1)-O) but zero-order reaction over the non-polar faces ZnO(1 0 −1 0) [29]. While Kislov and co-workers called them intriguing, their observations can be very well understood with our model: In fact their scenario is inverse analogous to our experiments: We changed the charge state of the dye (zwitterionic: zero-order; cationic: first-order) and kept the charge state of the photocatalyst constant (negatively charged), whereas Kislov et al. dealt with different facets of a photocatalyst (face of alternating ions: zero-order; only one type of ion: first-order) and kept the charge state of the dye constant (negatively charged).

Similar to the effects that are caused by varying the polarity of a facet of a photocatalyst, the effects of varying the polarity of the solvent might be understood: The polarity of the solvent influences both, the solvation of the reactant and the Debye length, which characterizes the scope of the surface charge of the photocatalyst, thus the solvent has a major influence on the adsorption behavior of the reactant. Indeed, it has been reported for classical heterogeneous catalysis that changing the solvent from polar to non-polar might lead to a complete change of the reaction order [30].

Sigmoidal degradation curves as shown in Section 3.3 have also been found by other researchers when monitoring the degradation reactions conducted in multi-component mixtures [31]. Reactants that showed a first-order degradation when being monitored separately, exhibited a sigmoidal decay if another, stronger adsorbing reactant was present [31]. This finding can also be explained with our view: As in this case the photocatalyst is blocked by the competing reactant, the degradation of the regarded reactant is less active in the first stage. During the reaction, the adsorption of the regarded reactant increases because more specific surface gets available while the competing reactant is more and more decomposed.

In Section 3.3 we have demonstrated that the degradation of the anionic dye methyl orange can be described similar to bacteria inactivation using the empiric Hom equation (Eq. (2)), due to their similar behavior. For this reason, degrading methyl orange in the anionic state might finally serve as a preliminary test to estimate the suitability of a photocatalyst for photodisinfection. Such a test is much simpler to conduct than real bacteria decomposition reactions.

4. Conclusions

We presented a favorable model system to study the electrostatics and pH-dependent kinetics of heterogeneous photocatalytic reactions: Nano-β-$SnWO_4$ as the photocatalyst is very suitable due its remarkable stability allowing for continuous *in situ* measurement and its almost pH-independent surface charge. The dyes disperse black 3 and methyl orange, on the other hand, can be adjusted to three different charge states (cationic, zwitterionic and anionic) by varying the pH value within the acidic milieu and have their parent structure in common. We found that, under these conditions, the reaction order of the degradation reaction is essentially dependent on the pH value – *i.e.*, on the electrostatic interaction of dye and photocatalyst – and is adjustable from first- (cationic dye, pH 2.1) over zero- (zwitterionic dye, pH 2.3) to a mixed-order (anionic dye, pH 6.8, sigmoidal decay).

Note that the kinetics of methyl orange have been discussed controversy so far, and have ascribed to be of first- [32] or of zero-order [33], as well. Ironically, the data in Refs. [32a,33] suggest that in fact, sigmoidal decays were obtained, but not identified, demonstrating the difficulty of clear-cut kinetic studies.

The results obtained here cannot be explained with the monomolecular L–H-mechanism, commonly applied in heterogeneous photocatalysis but confirm the *kinetic-order paradox* encountered by Aramendía et al. [9]. As an alternative, we suggest a new concept: In contrast to the existing approach we did not simplify the classical bimolecular L–H-mechanism, which is used in heterogeneous catalysis, to a monomolecular view but expanded it to a much more realistic multi-component view taking the electric double layer of the photocatalyst into account. Mathematically describable with well-established steady-state kinetics, this expanded view nevertheless also ends up with a readily solvable two-parameter equation and allows interpreting experimental data that have been conflicting or misunderstood, so far. This concept is of significance to various problems. This includes, for

instance: (1) the optimization of degradation reactions including reactions conducted in electrolyte containing media or in mixtures of various reactants, (2) the prediction of the decomposition of a specific reactant in the presence of competing reactants, and (3) the preferential reaction of an isomer, if the acidity of the regarded isomers differs. Furthermore, influences of the polarity of specific crystal facets of the photocatalyst or the polarity of the solvent have been discussed. The analogy of the degradation reaction of the anionic azo dye methyl orange and photocatalytic inactivation of bacteria has also been demonstrated. Finally, it has been shown that *weak* rather than *strong* adsorption may lead to zero-order kinetics, especially in the case of most relevant non-charged reactants representing commodities or serving as model compounds for persistent pollutants.

Altogether, the here suggested concept reconciles reported contradictions, allows for interpreting results that have been intriguing so far and may help to optimize the activity of known as well as of novel photocatalysts, especially, for specific purposes.

Acknowledgments

The authors are grateful to the Center of Functional Nanostructures (CFN) of the Deutsche Forschungsgemeinschaft (DFG) at the Karlsruhe Institute of Technology (KIT) for financial support. J.U. acknowledges the support of the Fund of the Chemical Industry (FCI) and of the German National Academic Foundation.

Appendix A. Supplementary data

Supplementary data associated with this article can be found, in the online version, at http://dx.doi.org/10.1016/j.apcatb.2012.07.037.

References

[1] X. Chen, L. Liu, P.Y. Yu, S.S. Mao, Science 331 (2011) 746–750.
[2] (a) S. Han, S.-H. Choi, S.-S. Kim, M. Cho, B. Jang, D.-Y. Kim, J. Yoon, T. Hyeon, Small 8–9 (2005) 812–816;
(b) S. Kohtani, S. Makino, A. Kudo, K. Tokumura, Y. Ishigaki, T. Matsunaga, O. Nikaido, K. Hayakawa, R. Nakagaki, Chemistry Letters 31 (2002) 660–661.
[3] J. Ungelenk, C. Feldmann, Chemical Communications 48 (2012) 7838–7840.
[4] (a) J. Ng, X. Wang, D.D. Sun, Applied Catalysis B: Environmental 110 (2011) 260–272;
(b) N.C. Castillo, A. Heel, T. Graule, C. Pulgarin, Applied Catalysis B: Environmental 95 (2010) 335–347.
[5] (a) K. Zhou, Y. Li, Angewandte Chemie International Edition 124 (2012) 622–635 (review);
(b) G. Liu, J.C. Yu, G.Q. Lu, H.M. Cheng, Chemical Communications 47 (2011) 6763–6783 (review).
[6] D. Friedmann, C. Mendive, D. Bahnemann, Applied Catalysis B: Environmental 99 (2010) 398–406.
[7] J. Jiang, G. Oberdörster, P. Biswas, Journal of Nanoparticle Research 11 (2009) 77–89.
[8] (a) J.M. Herrmann, Applied Catalysis B: Environmental 99 (2010) 461–468 (review);
(b) B. Ohtani, Chemistry Letters 37 (2008) 217–229 (review);
(c) J.M. Herrmann, Catalysis Today 53 (1999) 115–129 (review).
[9] M.A. Aramendía, J.C. Colmenares, S. López-Fernández, A. Marinas, J.M. Marinas, J.M. Moreno, F.J. Urbano, Catalysis Today 138 (2008) 110–116.
[10] (a) I.K. Konstantinou, T.A. Albanis, Applied Catalysis B: Environmental 49 (2004) 1–14 (review);
(b) N. Guettaï, H.A. Amar, Desalination 185 (2005) 427–437;
(c) C. Guillard, H. Lachheb, A. Houas, M. Ksibi, E. Elaloui, J.M. Herrmann, Journal of Photochemistry and Photobiology A: Chemistry 158 (2003) 27–36;
(d) H. Lachheb, E. Puzenat, A. Houas, M. Ksibi, E. Elaloui, C. Guillard, J.M. Herrmann, Applied Catalysis B: Environmental 39 (2002) 75–90;
(e) C.M. So, M.Y. Cheng, J.C. Yu, P.K. Wong, Chemosphere 46 (2002) 905–912.
[11] B. Neppolian, H.C. Choi, S. Sakthivel, B. Arabindoo, V. Murugesan, Chemosphere 46 (2002) 1173–1181.
[12] (a) J. Ungelenk, C. Feldmann, Applied Catalysis B: Environmental 102 (2011) 515–520;
(b) J. Ungelenk, C. Feldmann, Patent Application WO 2012031645.
[13] R.I. Bickley, Journal of Photochemistry and Photobiology A: Chemistry 216 (2010) 256–260.
[14] H. Al-Ekabi, N. Serpone, Journal of Physical Chemistry 92 (1988) 5726–5731.
[15] D.A. Walker, B. Kowalczyk, M. Olvera de la Cruz, B.A. Grzybowski, Nanoscale 3 (2011) 1316–1344 (review).
[16] C.S. Hanes, Biochemical Journal 26 (1932) 1406–1421.
[17] C. Tizaoui, K. Mezughi, R. Bickley, Desalination 273 (2011) 197–204.
[18] (a) A.M.T. Silva, E. Nouli, N.P. Xekoukoulotakis, D. Mantzavinos, Applied Catalysis B: Environmental 73 (2007) 11–22;
(b) H. Al-Ekabi, N. Serpone, Langmuir 5 (1989) 250–255.
[19] (a) M.J. Watts, A.T. Cooper, Solar Energy 82 (2008) 206–211;
(b) H. Tahiri, Y.A. Ichou, J.M. Herrmann, Journal of Photochemistry and Photobiology A: Chemistry 14 (1998) 219–226.
[20] H.C. Genuino, E.C. Njagi, E.M. Benbow, G.E. Hoag, J.B. Collins, S.L. Suib, Journal of Photochemistry and Photobiology A: Chemistry 217 (2011) 284–292.
[21] (a) G. Liu, P. Niu, C. Sun, S.C. Smith, Z. Chen, G.Q.M. Lu, H.M. Cheng, Journal of the American Chemical Society 132 (2010) 11642–11648;
(b) Y. Liu, Z. Wang, B. Huang, X. Zhang, X. Qin, J. Ying Dai, Journal of Colloid and Interface Science 348 (2010) 211–215;
(c) A.O. Ibadon, G.M. Greenway, Y. Yue, P. Falaras, D. Tsoukleris, Applied Catalysis B: Environmental 84 (2008) 351–355.
[22] (a) M.N. Chong, B. Jin, C.P. Saint, Chemical Engineering Journal 171 (2011) 16–23;
(b) M.N. Chong, B. Jin, H. Zhu, C.P. Saint, Journal of Photochemistry and Photobiology A: Chemistry 214 (2010) 1–9;
(c) J.A. Rengifo-Herrera, E. Mielczarski, J. Mielczarski, N.C. Castillo, J. Kiwi, C. Pulgarin, Applied Catalysis B: Environmental 84 (2008) 448–456;
(d) Y. Kan, C. Hu, Y. Hu, J. Qu, Applied Catalysis B: Environmental 73 (2007) 354–360.
[23] (a) O.K. Dalrymple, E. Stefanakos, M.A. Trotz, D.Y. Goswami, Applied Catalysis B: Environmental 98 (2010) 27–38 (review);
(b) J. Marugán, R. van Grieken, C. Sordo, C. Cruz, Applied Catalysis B: Environmental 82 (2008) 27–36;
(c) M. Cho, H. Chung, J. Yoon, Applied and Environment Microbiology 69 (2003) 2284–2291.
[24] D. Gumy, C. Morais, P. Bowen, C. Pulgarin, S. Giraldo, R. Hajdu, J. Kiwi, Applied Catalysis B: Environmental 63 (2006) 76–84.
[25] C. McCullagh, J.M.C. Robertson, D.W. Bahnemann, P.K.J. Robertson, Research on Chemical Intermediates 33 (2007) 359–375 (review).
[26] M. Szpakowska, I. Uruska, R. Teszner, Journal of Thermal Analysis 32 (1987) 717–728.
[27] Z. Rapoport (Ed.), CRC Handbook of Tables for Organic Compound Identification, 3rd ed., Boca Raton, Florida, Taylor & Francis, 1984.
[28] CRC Handbook of Chemistry, Physics, 73rd ed., CRC Press, Boca Raton, FL, 1993.
[29] N. Kislov, J. Lahiri, H. Verma, D.Y. Goswami, E. Stefanakos, M. Batzill, Langmuir 25 (2009) 3310–3315.
[30] A. Gamez, J. Köhler, J. Bradley, Catalysis Letters 55 (1998) 73–77.
[31] M.I. Franch, J.A. Ayllón, J. Peral, X. Domènech, Catalysis Today 76 (2002) 221–233.
[32] (a) A. Zhang, J. Zhang, Journal of Hazardous Materials 173 (2010) 265–272;
(b) X. Liu, C. Liang, H. Wang, X. Yang, L. Lu, X. Wang, Materials Science and Engineering 326 (2002) 235–239.
[33] G. Chen, G. Luo, X. Yang, Y. Sun, J. Wang, Materials Science and Engineering 380 (2004) 320–325.